Biomarker-free dielectrophoretic sorting of differentiating myoblast multipotent progenitor cells and their membrane analysis by Raman spectroscopy.

Biomicrofluidics 6, 034113 (2012)

Biomarker-free dielectrophoretic sorting of differentiating myoblast multipotent progenitor cells and their membrane analysis by Raman spectroscopy

Massimo Muratore[1], Vlastimil Srsen[2], Martin Waterfall[3], Andrew Downes[4], Ronald Pethig[1*].

[1] Institute for Integrated Micro and Nano Systems, [4] Institute for Materials and Processes, School of Engineering, The University of Edinburgh, Edinburgh EH9 3JF, UK

[2] Wellcome Trust Centre for Cell Biology, The University of Edinburgh, Edinburgh EH9 3JR, UK

[3] Institute of Immunology & Infection Research, School of Biological Sciences, The University of Edinburgh, Edinburgh EH9 3JR, UK

Myoblasts are muscle derived mesenchymal stem cell progenitors that have great potential for use in regenerative medicine, especially for cardiomyogenesis grafts and intracardiac cell transplantation. To utilise such cells for pre-clinical and clinical applications, and especially for personalized medicine, it is essential to generate a synchronised, homogenous, population of cells that display phenotypic and genotypic homogeneity within a population of cells. We demonstrate that the biomarker-free technique of dielectrophoresis (DEP) can be used to discriminate cells between stages of differentiation in the C2C12 myoblast multipotent mouse model. Terminally differentiated myotubes were separated from C2C12 myoblasts to better than 96% purity, a result validated by flow cytometry and Western blotting. To determine the extent to which cell membrane capacitance, rather than cell size, determined the DEP response of a cell, C2C12 myoblasts were co-cultured with GFP-expressing MRC-5 fibroblasts of comparable size distributions (mean diameter ~10 μm). A DEP sorting efficiency greater than 98% was achieved for these two cell types, a result concluded to arise from the fibroblasts possessing a larger membrane capacitance than the myoblasts. It is currently assumed that differences in membrane capacitance primarily reflect differences in the extent of folding or surface features of the membrane. However, our finding by Raman spectroscopy that the fibroblast membranes contained a smaller proportion of saturated lipids than those of the myoblasts suggests that the membrane chemistry should also be taken into account.

[*] Author to whom correspondence should be addressed. Electronic mail: Ron.Pethig@ed.ac.uk

I. INTRODUCTION

Myoblasts, a mesenchymal stem cell derived precursor, have the ability to differentiate into diverse cell lineages by means of chemical cues and/or co-factors present in the culture media[1,2]. These multipotent characteristics and the availability of these cells make them amenable for regenerative medicine applications. Several studies have reported the use of these cells for cardiomyogenesis grafts[3], intracardiac cell transplantation[4,5] and also early pre-clinical studies have shown successful implantation in human patients with ischemic heart failure[6,7]. Although the initial reports appear promising there is scant information about the optimal differentiation status[5,8] and how to distinguish the phenotypical and physiological variations in a population of cells for implantation. The work reported here demonstrates that these issues may possibly be addressed using dielectrophoresis (DEP).

Traditional methods such as flow cytometry identify and characterise specific cell attributes by utilising labelled antibodies to specific biological markers that may change the physiology of the cells selected, rendering further medical applications challenging. DEP, as recently reviewed[9-12] is a biomarker-free technique that utilises the induced dynamic response of a cell to imposition of a non-uniform radio-frequency electric field. For a particular field frequency, the DEP response of a cell depends on whether its intrinsic dielectric polarisability is less or greater than that of its surrounding suspending medium. For the range of field frequencies and experimental conditions used in this study, the observed dynamic response is characterised either by the cell moving up a field gradient towards an electrode (positive DEP) or down a field gradient away from an electrode (negative DEP). The transition between these types of DEP response corresponds to where the effective polarisability of the cell equals that of the surrounding medium and occurs at the so-called DEP cross-over frequency f_{xo}. For a spherical cell of radius r this frequency is given to good approximation by:

$$f_{xo} = \frac{\sqrt{2}\sigma_m}{2\pi r C_m} \qquad (1)$$

In this equation C_m is the specific capacitance (capacitance per unit area) of the cell membrane, σ_m is the conductivity of the suspending medium, and the assumption is made that the high resistance to passive ion flow across the membrane has not been impaired due to the onset of cell death or physical damage, for example[13]. The protocols for obtaining the cell separations reported here relied on the different cell types (C2C12 myoblasts, myotubes and MRC-5 fibroblasts) exhibiting different f_{xo} values. This can reflect differences in either or both their average cell size or membrane capacitance. A cell's plasma membrane acts as a capacitor because it is constructed like one - namely a thin dielectric shell situated between two conductors (the outer and inner electrolytes). It is customary to employ the low-frequency (DC) approximation[14] to analyse the dielectric and conductive properties of a cell, so that for a spherical cell of measured radius r the effective permittivity ε_{eff} of a cell is given by:

$$\varepsilon_{eff} = \frac{\varepsilon_o \varepsilon_m r}{\delta} \phi_m = rC_m \qquad (2)$$

where δ is the membrane thickness, ε_o the permittivity of free space, and ε_m is the mean relative permittivity of the material forming the membrane structure. The factor ϕ_m in equation (2) is termed the membrane-folding factor to take into account cell surface features such as folds, microvilli, ruffles and blebs[15]. For a perfectly smooth spherical cell $\phi_m = 1$. The DEP measurements reported here did not extend above 700 kHz, a suspending medium conductivity of 120 mS/m was used, and high cell viabilities were maintained during their DEP separations. Under these conditions the low-frequency approximation used in equation (2) leads to an accurate measurement of the membrane capacitance[16]. Labeed *et al*[17] have recently reported that the neurogenic potential of human neural stem/progenitor cell populations can be discriminated by their f_{xo} and derived C_m values. On the basis of the efficient DEP-based cell separations reported here, the same conclusion may be reached regarding discrimination between stages of C2C12 myoblast cell differentiation.

In the DEP literature[9, 13, 15] it has been assumed that the value of C_m primarily depends on the extent of membrane folding as given by ϕ_m. One of the objectives of this work

was to investigate to what extent the chemical composition of the membrane might also influence its specific capacitance value. Raman spectroscopy has previously been used to investigate chemical changes associated with the differentiation of stem cells[18-20], as well as an on-chip detection method for monitoring the DEP separation of bacteria[21]. In this work we have used Raman spectroscopy to determine how differences in the molecular composition of the membranes of two cell types of similar size, namely C2C12 myoblasts and MRC-5 fibroblasts, might correlate with their observed DEP responses and derived C_m values.

II. MATERIALS AND METHODS

All the chemical and reagents were purchased from Sigma (Poole, UK) unless otherwise stated.

A. Cell cultures

i) C2C12 mouse myoblast cell line:

Cells were plated at a density of 3000 cells/cm² and grown in high glucose DMEM growth medium (GM) supplemented with 10% FBS (HyClone), 2 mM of L-glutamine, 100 units/ml of penicillin and 100 μg/ml streptomycin sulphate (Invitrogen). Cells were passaged every two days at a ratio of 1:9 and they were induced to myogenic differentiation at 90% confluence. The differentiation medium (DM) was composed of high glucose DMEM, 0.1% FBS (Hyclone), 100 units/ml of penicillin and 100 μg/ml streptomycin sulphate (Invitrogen), 5 μg/ml transferrin and 10 μg/ml insulin. The DM was changed every other day. All cultures were kept at 37ºC with 5% CO_2. C2C12 myoblasts differentiate and fuse into phenotypically distinct elongated multinuclear myotubes that express embryonic myosin[22, 23].

Images are given in Figure 1 of a C2C12 culture at the time (day 1) of seeding; at the first stage of myotube formation 2 days after induction (on day 2 after seeding); at the stage (day 7 after induction) where the cells were prepared for DEP separation.

ii) MRC-5-GFP fibroblasts:

The cells were cultured in the same GM as C2C12, and were further supplemented with 2 μl/ml puromycin to maintain selection pressure, as well as green fluorescent protein (GFP) expression. The cells were passaged every two days at a ratio of 1:4.

iii) Co-culturing:

To characterise the DEP properties of cells of a similar size (~ 10 μm diameter), MRC-5-GFP fibroblasts were used as a feeder layer for co-culturing C2C12 myoblasts. The medium for both cell types was GM supplemented with 2 μg/ml of puromycin (to select for GFP expression) and cultured for a week before analysis. Because of the GFP expression the MRC-5-GFP fibroblasts and C2C12 myoblasts could readily be identified by flow cytometry.

B. Flow Cytometry

Samples were analysed using a LSRII flow cytometer (Beckton Dickinson Immunocytometry Systems, UK) running BD FACSDiva v6 Software. An electronic acquisition gate was applied to the forward/side scatter (FSC/SSC) plot to exclude debris from intact material and typically more than 50,000 events were acquired in this gate. GFP or Alexa Fluor® 488 conjugated secondary antibody binding was detected using 488 nm laser excitation and a recording of fluorescence in the range 500-550 nm. Analysis was performed using FlowJo software (Tree Star, USA). Debris was excluded through FSC/SSC profile gating before applying electronic gates to assess green fluorescence. Sort purity was calculated through gating based on profiles from each cell type as controls.

For analysis of myotubes, cells were collected separately from the central and outer exit ports of the DEP chamber and washed in PBS (Mg^{++}-, Ca^{++}-free) supplemented with 0.1% BSA fraction V and 0.1% NaN_3. The cells were centrifuged at 350 g for 5 minutes and the pellet was re-suspended and fixed in 2% formaldehyde solution for 10 minutes at room temperature. The fixed cells were washed in permeabilisation buffer (PB) composed of PBS (Mg^{++}-, Ca^{++}-free) supplemented with 0.1% BSA V, 0.1% NaN_3 azide and 0.1% saponin (S-7900). Primary antibodies for embryonic myosin (specific for myotubes) were diluted in 100 μl of PB for incubation with the cell samples for 90 minutes at 4^0C. After primary antibody incubation cells were centrifuged and washed in a single large volume (3ml) of PB. Secondary antibodies, conjugated with Alexa Fluor® 488, were added to cells suspended in PB and

incubated for another 90 min at 4^0C. Finally, the cells were re-suspended in 400 µl of F-PBS and flow cytometry analysis performed.

For C2C12 myoblasts co-cultured with MRC-5-GFP fibroblasts, the separation performance by DEP was assessed by flow cytometry. The cells were collected separately from the two exit ports of the DEP chamber and washed in Flow-PBS (F-PBS) composed of PBS (Mg^{2+}, Ca^{2+} free) supplemented with 0.1% NaN_3 and 0.2% BSA V prior to acquisition.

Propidium iodide (PI), which is membrane impearmeable and excluded from viable cells, was used as a fluorescent DNA stain to evaluate cell viability after DEP separation. Immediately prior to cell acquisition for viability, 10µl PI solution (50µg/ml PI + 100µg/ml RNase in PBS) was added directly to sample tubes and staining detected using 488 nm laser excitation and recording of fluorescence in the range 633-677 nm . Viability was calculated through gating based on profiles from unstained samples.

C. DEP studies

Details of the design and basic operation of the DEP chamber used for the cell separations are shown in Figures 2 and 3. The 'fishbone' quadrupole geometry of the electrodes is a modified version of designs incorporated into DEP cell manipulation and separation devices described by other laboratories[21,24-28]. Following the procedure described by Hu *et al*[26] the cell mixture (~$4x10^6$ cells/ml) entered the chamber through two ports at the sides of the chamber. The widths of these two flow streams were ~440 µm. Buffer fluid of the same conductivity as that used to suspend the cell mixture was introduced into the chamber through a centre port, to produce a cell-free central stream of width ~120 µm. The selective separation of target cells from a mixture was achieved by steadily deflecting them by negative DEP from the outer laminar flow streams into the central fluid stream. As depicted in Figure 3 other cells remained in the two outer fluid streams, either because they did not experience a sufficiently strong negative DEP force to overcome the hydrodynamic force, or a positive DEP force attracted them towards the electrodes. The electrodes (~0.2 µm) were sufficiently thin compared with the fluid channel height (100 µm) that their

influence on the laminar flow profile in the chamber was negligible. Tests were also made to confirm that, with no voltage signal applied to the electrodes, cells injected into the two side ports were carried through the chamber with no observable diffusion into the central fluid stream. The final design of the chamber resulted from tests and successive modifications of various prototypes, some of which are described in section III.B.

Platinum (200 nm thick) electrodes were sputtered onto a seed layer of titanium (20 nm) on glass substrates using standard photolithography and lift-off techniques. The electrodes, each of width 15 μm and spaced 500 μm apart, were grouped into three equally spaced sets of five quadrupole 'funnel' arrays angled at 18^{o} to the direction of intended fluid flow (see Figure 3). The gap between the tips of adjacent (coplanar) electrodes was 100 μm for the first set of five quadrupoles to be located next to the fluid inlet ports, and this was reduced to 75 and then 50 μm for the next two sets. The fluidic chamber, length 9.4 mm, height 100 μm and width 1 mm, was fabricated by patterned photolithography with SU-8. The two glass substrates were bonded to face each other onto the SU-8 fluidic framework, using alignment marks to ensure close (± 2 μm) matching of the upper and lower sets of electrodes. By this means a total of 15 quadrupole 'funnel' electrode arrays were established along the length of the DEP chamber. The chamber was mounted onto a custom made holder for fluidic and electrical connections (Figure 2), and two syringe pumps (Harvard Apparatus) were used for the separate pumping of the DEP fluid medium (without cells) and cell suspensions into the chamber. Cells were collected at room temperature (~294K) from the two outlet ports for further analysis. Prior to use, the DEP chamber was filled with 20% BSA for 10 min and then flushed through with 70% ethanol - a procedure adopted to reduce cell adhesion to the chamber walls and the formation of air bubbles, respectively. For the DEP cell separations reported here a volumetric flow rate of 120 μl/h was established for periods of 2~3 hours, so as to collect at least ~$5x10^{5}$ cells from the exit fluidic ports for flow cytometry analysis. The conductivity of the DEP medium was adjusted to ~120 mS/m with osmolarity calculated at ~330 mOsm/kg. Sinusoidal voltages of 10 V(pk-pk) were applied to the electrodes over the frequency range 150 - 700 kHz using an Agilent/HP 3325A function generator.

D. Western Blotting:

Myoblasts and myotubes were mixed prior to sorting by the DEP device and the separated fractions were collected for Western blot analysis. Cells were centrifuged at 250 g and re-suspended in cold PBS. The suspension was centrifuged at 350 g for three minutes and the pellet was re-suspended in three parts of distilled water and one part of 4x NuPAGE-SDS Sample Buffer (Invitrogen) supplemented with 10% of β-Mercaptoethanol. The samples were denatured by boiling for six minutes. Proteins were resolved by 6% SDS-PAGE and transferred to a nitrocellulose membrane (LI-COR Bioscience). The membrane was blocked in 5% milk in TBS containing 0.1% Tween 20 over night. The blocking procedure was followed by one hour incubation with antibodies against embryonic myosin (EMHC, clone F1.652, developed by Helen Blau, University of Iowa) diluted 1:1000 and anti-α tubulin antibody diluted 1:5000 (clone B-5-1-2 Sigma). The primary antibody was detected with secondary IR800 conjugated goat anti-mouse antibody (LI-COR Bioscience) at room temperature for 2 hours. Visualisation of the signal was performed using a LI-COR Odyssey near-infrared scanner and Odyssey 3.0,16 software with median background subtraction.

E. Plasma membrane purification

Plasma membranes from C2C12 myoblasts, myotubes and MRC-5-GFP fibroblasts were purified by a two-phase partition process[29] except that cell disruption was achieved by homogenisation with a dounce and pestle pre-chilled at -20^0C. The plasma membrane preparations from all three cell types were collected and dried under a stream of nitrogen before Raman spectroscopy.

F. Raman spectroscopy

Raman spectra were obtained using a Renishaw inVia Raman microscope (785 nm near-IR laser excitation, 40 mW at sample) with a 40x objective lens and 0.75 numerical aperture. The membranes were deposited onto a quartz substrate (SPI Supplies), dried under a stream of nitrogen and positioned on the inverted stage of the microscope. Each spectrum was acquired over approximately 2 minutes for six samples obtained from the membranes of the C2C12 myoblasts, myotubes and MRC-5-GFP fibroblasts. Principal component analyses (PCA) were performed for six separate spectra obtained from the membranes of each of the three cell types (C2C12

myoblasts, myotubes and MRC-5-GFP fibroblasts). PCA is an analytical procedure[30] that aids the identification of the principle differences between samples by translating a high number of possibly correlated variables into a smaller number of uncorrelated principal components. This exercise was undertaken to determine how differences in the molecular composition of the membranes of the different cell types might correlate with their observed DEP responses and derived C_m values.

III. RESULTS

A. Flow Cytometry

Immediately after harvesting the cells were transferred into DEP medium, pumped into the DEP chamber and the cell populations eluted from the central and side flow streams were collected for analyses by flow cytometry. Purity of the recovered sub-populations was assessed based on either the intrinsic GFP expression of the MRC-5 fibroblasts or staining for myotubes with anti-embryonic myosin antibody, detected using a secondary Alexa Fluor® 488 antibody. Analyses of cell mixtures that had been pumped through the DEP chamber with no voltages applied to the electrodes are shown in Figure 4(a), and were used to determine the appropriate gating strategy for flow cytometry evaluation of DEP separated sub-populations. The DEP separation and analysis by flow cytometry was performed for 13 separate samples of each paired combination of the three cell types, with the results expressed as percentages of cells that were determined by flow cytometry to be positive for GFP or Alexa Fluor 488, or fluorescence negative.

The forward scatter plots obtained for C2C12 myoblasts (n = 59,518) and MRC-5-GFP fibroblasts (n = 23,343) are shown superimposed in Figure 4(b). Under microscopic inspection (x200) these two cell types appeared to be of closely similar size (~10 μm diameter) and size distribution, and this conclusion is supported by the forward scatter data. The results shown in Figure 4(b) give median FSC-A values of 98.05 K and 86.72 K for the C2C12 and MRC-5 cells respectively, with median absolute deviations of 47.1% and 55.7%, respectively (the median, rather than mean, is generally used in flow cyotmetry as data rarely has a symmetrical unimodal distribution). These results indicate that, although there was a relatively small difference in their average size, the C2C12 and MRC-5 cells exhibited almost

completely overlapping size distributions. The observed large biological varience in morphological size is not unusual. Based on this FSC data and the estimated average cell size of 10 μm diameter for their mixtures, the C2C12 cells were estimated on average as 13% larger in diameter and of a more narrow size distribution than the MRC-5 cells.

B. DEP cell separations

Initial considerations of the design and testing of the DEP device included an estimation of the optimal rate of fluid flow through the chamber. The electrodes direct a cell into the central flow stream when the negative DEP force acting on it exceeds the Stokes hydrodynamic drag force. Adopting the effective dipole moment approximation[9] for the time-averaged DEP force acting on a spherical particle of radius *r*, this condition can be expressed as

$$2\pi\varepsilon_o\varepsilon_{fl} r^3 \,\mathrm{Re}(CM)\nabla E^2 > 6\pi\eta v r \sin\theta \qquad (4)$$

where ε_{fl} is the relative permittivity (~79) of the aqueous suspending fluid, Re(*CM*) is the real part of the Clausius-Mossottti factor that quantifies the effective polarizability of the particle, *E* is the rms value of the applied electric field, η is the dynamic viscosity of the fluid, *v* is the fluid velocity, and θ is the angle (18^o) at which the electrodes were set against the direction of fluid flow. The *CM* factor is bounded by the limits -0.5 < Re(*CM*) < 1.0, and as a first approximation it was assumed that an Re(*CM*) vaue of -0.2 is sufficient to achieve the required negative DEP force for a cell to be deflected from the outer flow streams towards the central one. From equation (4), for a cell of radius 5 μm in an aqueous fluid ($\eta = 10^{-3}$ Pa.s) and electrodes angled at $\theta = 18^o$, the minimum value of ∇E^2 required to direct cells into the central fluid stream is:

$$\nabla E^2 > 2.1\times10^{19} v \quad (\mathrm{V^2/m^{-3}}) \qquad (5)$$

Approximating the fluidic chamber as two smooth infinite parallel plates, and assuming the flow to be laminar, the fluid velocity $v(x)$ as a function of height x above the chamber floor is given by[31]:

$$v(x) = 6\bar{v}\left[(x/h) - (x/h)^2\right] \qquad (6)$$

where $\bar{v}$ is the mean flow velocity. For a channel height h = 100 μm, $v(x) = \bar{v}$ at x = 14.6 μm. Values for the field gradient and ∇E^2 generated by a single quadrupole electrode structure were determined using COMSOL Multiphysics (version 3.5) software, and this indicated that values for ∇E^2 of the order $5\text{x}10^{15}$ V^2/m^3 are created at a distance of 14.6 μm above the electrode edges with an applied voltage of 10 V(pk-pk). From equation (5) this provided, for the case of a single quadrupole array and an applied voltage of 10 V(pk-pk), the guideline of ~2.4 x 10^{-4} m/s as the maximum fluid velocity to be used to achieve deflection of cells passing to within ~15 μm of an electrode edge. For the DEP chamber cross-section of 100 μm x 1 mm, this corresponded to a maximum volumetric flow rate of ~86 μl/hr for the case of one electrode array. After testing several prototypes, the strategy adopted to achieve maximum cell separation purity was to employ a volumetric flow rate of 120 μl/hr with 15 quadrupole electrode arrays in the chamber (compared to the three electrode arrays used by Hu *et al*[26]).

C2C12 myoblasts were passaged and differentiated into myotubes as described in section II.A. From 40% to 70% of C2C12 myoblasts differentiated into myotubes, depending on passage number of the cells. To determine the voltage frequency for the most efficient cell separation, cell samples were pumped through the DEP chamber for a range of frequencies, commencing at 150 kHz, and samples collected from the exit ports were analysed by flow cytometry. Results obtained for a sample containing C2C12 myoblasts, 9 days after plating and 7 days after induction to produce myotubes, are shown in Figure 5. DEP separation performed at 150 kHz resulted in elution of a mixture of C2C12 myoblasts and myotubes from the central flow stream. However, as shown in Figure 5(a), with increasing voltage frequency the ratio of C2C12 myoblasts to myotubes collected from the central port increased, until at 400 kHz about 95% of the cells collected from the central port were C2C12

myoblasts. This result indicates that for frequencies in the range 350-400 kHz the myotubes were either close to their average DEP cross-over (f_{xo}) frequency or experienced a weak positive DEP force. As shown in Figure 4(b) 98.6% of the cells collected from the outer flow streams at 409 kHz were myotubes (positive to the Alexa Fluor® 488 probe) and, as indicated in Figure 4(c), the C2C12 viability was typically around 96% after DEP separation. Variable, better than 65%, viability was determined for the DEP separated myotubes. The undifferentiated C2C12 myoblasts can be expected to be far less sensitive to environmental change than the contractile differentiated myotubes. A highly efficient separation of the C2C12 myoblasts from the differentiated myotubes with limited viability loss had therefore been achieved at 409 kHz. Above 409 kHz the number of C2C12 cells collected from the central port decreased, until at 670 kHz very few cells appeared in the central flow stream. This frequency can be considered to be close to f_{xo} for the C2C12 myoblasts.

As an additional validation of the efficient separation by DEP of C2C12 myoblasts from myotubes, a Western blot analysis for the marker embryonic myosin was performed. This protein is only present in the late phase of development from C2C12 myoblasts to differentiated myotubes[22, 23]. The cells were mixed and sorted by DEP at 400 kHz, and samples collected from the centre and outer flow ports were analysed as described in section II.D for embryonic myosin. Tubulin-α was used as loading control to calibrate for protein content. The results given in Figure 6 show that the only cells positive for embryonic myosin were those collected from the outer flow port, and that none of this protein was detected in the sample obtained from the centre port of the DEP chamber. This finding is compatible with the results shown in Figure 5. Although this is a less quantitative method than flow cytometry, it provided further validation of the high level of cell separation achieved using the DEP chamber design and protocol described here.

A 409 kHz separation of C2C12 myoblasts from myotubes was used to produce pure populations of these cells for tests of the DEP separation of C2C12 co-cultured with MRC-5-GFP cells, and of myotubes mixed with MRC-5-GFP cells. Where possible, depending on their concentrations after DEP sorting, roughly equal numbers of cells were used to prepare heterogeneous samples of myotubes with the MRC-5-GFP cells.

Mixing of the C2C12 myoblasts and MRC-5-GFP fibroblasts before DEP separation was not required as the MRC-5 feeder cells were co-cultured with C2C12 cells. The flow cytometry control experiments for setting the appropriate gating for these samples are shown in Figure 4. The results leading to the best DEP separation of C2C12 co-cultured with MRC-5-GFP are given in Figure 7, and indicate that f_{xo} for the MRC-5-GFP fibroblasts was close to 500 kHz. At this frequency 99.9% of the cells collected from the centre port were C2C12 myoblasts, and the MRC-5-GFP cells accounted for 97.7% of the cells collected from the outer port. Based on flow cytometry data after PI cell staining, cell viabilities were typically found to be above 97%. The results associated with the most efficient separation of a mixture of myotubes and MRC-5-GFP fibroblasts are shown in Figure 8. From these results it can be deduced that f_{xo} for myotubes was close to 400 kHz, at which frequency 100% of the cells collected from the centre port were determined to be MRC-5-GFP fibroblasts, whilst 99.1% of the cells eluted from the outer port were myotubes.

C. Raman spectroscopy

The spectra obtained for membrane samples extracted from the C2C12 myoblasts and MRC-5-GFP fibroblasts are shown in Figure 9. The most significant differences in membrane chemistry are indicated by the vibrational frequency ranges 1 and 2, corresponding to CH_2 and CH_3 bending (1300 - 1500 cm^{-1})[32-34] and stretching for saturated long CH chains (2800 - 2950 cm^{-1})[35-37]. A principle component analysis of the Raman spectra shown in Figure 9 was performed. Vibrational spectra were obtained for six samples of each type of cell membrane. The best separation between the three membrane type was achieved when the principal component 3 (PC3) was plotted against principal component (PC2) as illustrated in figure 10. PC3 was associated, after data analysis, to be responsible for changes in lipid saturation in the membranes. Thus, the content of saturated hydrocarbon bonds (vibrational frequencies of 1296, 1440, 1460, 2880 cm^{-1}) was determined to be larger for the C2C12 myoblasts than for the MRC-5 fibroblasts, and the unsaturated hydrocarbon (1660 cm^{-1}) content was determined to be less for the MRC-5 fibroblasts than for the C2C12 myoblasts. The scatter plot shown in Figure 10 indicated that the PC2 and PC3 components gave the best separation between the three cell types, confirming the conclusion drawn from the Raman spectra shown in Figure 9 that the C2C12 myoblast membranes contained the largest relative proportion of saturated lipid

bonds. The myotube membranes contained a smaller content of saturated hydrocarbon bonds than either the C2C12 or MRC-5 cells.

IV. DISCUSSION

A total of 39 mixed-cell samples were processed through the DEP chamber at a flow rate of 120 μl/hr and an applied voltage of 10V (pk-pk), comprising thirteen separations at 409 kHz of C2C12 cells from their differentiated myotubes; C2C12 and MRC-5 co-cultured cells separated at 500 kHz; myotube and MRC-5 cell mixtures separated at 400 kHz. The results shown in Figures 5, 7-8 represent the best separation purities obtained in these experiments. Overall, the following mean separation purities obtained were: 96.16 ± 3.03% (C2C12 myoblasts, n = 26); 98.9 ± 0.63% (MRC-5-GFP fibroblasts, n = 26) and 97.0 ± 1.9% for myotubes (n = 26).

A factor contributing to these highly efficient cell separations was the decision, by adopting a relatively low rate of fluid flow, to strive for output purity rather than high sample throughput. The flow rate 120 μl/hr corresponded to a mean fluid velocity of 330 μm/s, so that the average time t taken by a cell to flow through the chamber (length 9.4 mm) was 28.5 s. The mean displacement of the cells by Brownian diffusion during this time, in the absence of a DEP force, is $\sqrt{2Dt}$ where D is the cell diffusion coefficient given by the Stokes-Einstein equation:

$$D = kT/(6\pi\eta r) \qquad (7)$$

with k the Boltzmann constant, T temperature, η the fluid viscosity and r the hydrodynamic radius of the cell. From equation (7) the diffusion coefficient for a cell of radius ~ 5μm at room temperature in an aqueous solution (η = 1 x 10^{-3} Pa) is ~4 x 10^{-14} m^2s^{-1}. After 28.5 seconds the mean displacement ($\sqrt{2Dt}$) of a cell by diffusion was thus ~1.5 μm. Contamination arising solely from the Brownian diffusion of non-target cells into the 50 μm wide 'funnel' leading up to the central output fluid port would therefore have been extremely low for our experiments. Also, the sedimentation velocity v_s of a cell, in the absence of a significant DEP force, is

determined by the balance of the Stokes drag force against the gravitational settling force:

$$6\pi\eta r v_S = (4/3)\pi r^3 \Delta\rho g \qquad (8)$$

where $\Delta\rho$ is the difference in density between the cell and suspending fluid, and g is the gravitational constant. Based on the density of 1.08 g/cm^3 reported for lymphocytes[38] and the density (1.02 g/cm^3) of the DEP medium, v_s can be estimated as ~3 μm/s[1]. Even in the absence of a negative DEP force driving cells downward from the upper plane of electrodes, there was thus a high probability that cells passing through the chamber would sediment down to the lower electrode plane and thereby not escape strong DEP forces.

The frequency dependencies of the Clausius-Mossotti polarizability functions Re(*CM*) for the three cell types can be derived, based on their estimated DEP cross-over (f_{xo}) values. Using the standard form of Re(*CM*)[9,13,15] modelling was performed using Matlab (The Maths Works Inc.) and the results are shown in Figure 11. These curves for Re(*CM*), limited to the region around the range of f_{xo} values for the three cell types, assist an understanding of the frequency dependencies and DEP separations shown in Figures 5, 7-8. The large difference of ~300 kHz between the average f_{xo} values for the C2C12 myoblasts and myotubes, and that of ~200 kHz for the C2C12 and their feeder MRC-5-GFP cells, would have been a factor leading to their efficient separation by DEP. The fact that good separations were also obtained for mixtures of myotubes and MRC-5-GFP fibroblasts suggests that there was a negligible overlap of their f_{xo} distributions about their mean values of around 400 kHz and 500 kHz, respectively. The C2C12 myoblasts and MRC-5-GFP fibroblasts were observed, using a microscope (x200), to be of near spherical shape and of roughly equal diameter (~10 μm). As shown in Figure 4(b) these two cell types exhibited closely matching flow cytometry forward scatter plots, indicating that their size distributions were of a similar lognormal form, skewed to larger cell sizes. Taking the average diameter of the two cell types to be 10 μm, and approximating the lognormal distributions shown in Figure 4(b) to be normal ones, the diameters of the C2C12 myoblasts and MRC-5-GFP fibroblasts can be estimated as 10.6 ± 3.1 μm and 9.4 ±

3.3 μm, respectively. Based on a medium conductivity of 120 mS/m and their estimated f_{xo} values of 700 kHz and 500 kHz, respectively, membrane capacitance values of 7.3 ± 3.0 mF/m^2 and 11.5 ± 5.3 mF/m^2 can be estimated for the C2C12 myoblasts and MRC-5-GFP fibroblasts, respectively. This suggests that the DEP separation of the similar sized C2C12 and MRC-5 cells was mainly associated with the difference in their membrane capacitance. The myotubes were of an elongated and convoluted shape, roughly three-times larger in volume than the C2C12 and MRC-5-GFP cells. The derivation of the membrane capacitance using equation (1) is only valid for spherical cells[9]. Whereas the polarizability of ellipsoids and truncated cylinders can be determined[39], the ill-defined shape of the myotubes prevents an estimation to be made of their membrane capacitance.

The results shown in Figures 9 and 10 indicate that the MRC5 fibroblasts contained a lower proportion of saturated hydrocarbon bonds than those of the C2C12 membranes. Lipid bilayers formed of saturated 'rigid' hydrocarbon chains will be thicker than those composed of unsaturated 'kinked' chains. Several explanations of the differences found in membrane chemistry are possible, but if the Raman data is interpreted as the MRC-5 cells having the thinner membrane, then based on equation (2) this would contribute to the finding that the MRC-5 cells possessed the larger membrane capacitance. Also, the relative permittivity of fatty acids decreases with increasing saturation. Examples include linolenic acid ($C_{17}H_{29}COOH$), linoleic acid ($C_{17}H_{31}COOH$), and oleic acid ($C_{17}H_{33}COOH$), respectively, with 25^{o}C relative permittivies of 2.54, 2.44 and 2.38, respectively[40]. This again could contribute to the MRC-5-GFP fibroblasts exhibiting a larger membrane capacitance compared to the C2C12 myoblasts. Therefore, membrane capacitance values derived from DEP experiments should be considered to reflect both the membrane chemistry (with interpretations regarding membrane thickness and dielectric polarizability), as well as a measure of the relative value of the membrane-folding factor ϕ_m.

V. CONCLUSIONS

High purities (>96%) of continuous DEP cell separation, with limited loss of cell viability, were obtained for myotubes terminally differentiated from C2C12 myoblasts, and for C2C12 myoblasts co-cultured with MRC-5 fibroblasts. These cell

separations were achieved using a modified form of the DEP chamber and electrode arrangement described by Hu *et al*[26]. The major modification was to increase (from two to fifteen) the number of quadrupole 'funnel' electrode arrays arranged along the length of the DEP chamber. The fact that the distribution of DEP cross-over frequencies (f_{xo}) were well separated for the three cell types was essential in leading to the high purities of cell separations. DEP forces acting alone are not capable of selectively discriminating to high purity different cells types that have an overlapping distribution of f_{xo} values.

Because of the irregular shape of the myotubes, it was not possible to assess the relative contributions that membrane capacitance and cell size make regarding the different values for f_{xo} exhibited by the C2C12 myoblasts and the myotubes. However, because of their similar size and shape the high purity DEP separation of co-cultured C2C12 and MRC-5 cells could be attributed to differences in their membrane capacitance values. Furthermore, based on the Raman spectra obtained for the membranes of these two cell types it was concluded that, apart from the membrane-folding factor ϕ_m, membrane thickness and molecular composition may also contribute to the specific membrane capacitance of a cell. Further investigations of this will be important in understanding how the DEP characteristics of stem cells change with differentiation, for example. In this work we have used Raman spectroscopy because it offers a direct and non-invasive method of obtaining structural, packing, and dynamic properties of membrane systems[41, 42]. In future work we will also exploit the ability of high resolution mass spectroscopy to provide quantitative analysis of complex membrane lipid mixtures at the subpicomole level, down to sample amounts of 1000 cells[43, 44].

ACKNOWLEDGMENTS

We thank Dr Borja Barredo for his assistance with the fabrication of the DEP chamber, Joe Burrage of the Wellcome Trust Centre for Cell Biology for his donation of the MRC-5-GFP fibroblasts, Dr Alistair Elfick for use of his Raman spectrometer, and Kay Samuel of the Scottish National Blood Transfusion Service, Royal Infirmary of Edinburgh, for her valuable advice. This work has been supported by the Edinburgh Research Partnership in Engineering and Mathematics.

REFERENCES

[1] S. Chen, S. Takanashi, Q. Zhang, W. Xiong, S. Zhu, E. C. Peters, S. Ding and P. G. Schultz, PNAS **104** (25), 10482 (2007).

[2] Y. Xu, Y. Shi and S. Ding, Nature **453** (7193), 338 (2008).

[3] G. Y. Koh, M. G. Klug, M. H. Soonpaa and L. J. Field, J. Clinical Investigation **92** (3), 1548 (1993).

[4] R. B. Thompson, S. M. Emani, B. H. Davis, E. J. van den Bos, Y. Morimoto, D. Craig, D. Glower and D. A. Taylor, Circulation **108** (10 suppl 1), II-264 (2003).

[5] X. L. Aranguren, J. D. McCue, B. Hendrickx, X.-H. Zhu, F. Du, E. Chen, B. Pelacho, I. Peñuelas, G. Abizanda, M. Uriz, S. A. Frommer, J. J. Ross, B. A. Schroeder, M. S. Seaborn, J. R. Adney, J. Hagenbrock, N. H. Harris, Y. Zhang, X. Zhang, M. H. Nelson-Holte, Y. Jiang, A. D. Billiau, W. Chen, F. Prósper, C. M. Verfaillie and A. Luttun, J. Clinical Investigation **118** (2), 505 (2008).

[6] S. Dimmeler, A. M. Zeiher and M. D. Schneider, J. Clinical Investigation **115** (3), 572 (2005).

[7] P. Menasché, A. A. Hagège, M. Scorsin, B. Pouzet, M. Desnos, D. Duboc, K. Schwartz, J.-T. Vilquin and J.-P. Marolleau, The Lancet **357** (9252), 279 (2001).

[8] B. C. Heng, T. Cao, H. K. Haider, A. J. Rufaihah and E. K.-W. Sim, Scandinavian Cardiovascular Journal **39** (3), 131 (2005).

[9] R. Pethig, Biomicrofluidics **4** (2), 022811 (2010).

[10] J. Regtmeier, R. Eichhorn, M. Viefhues, L. Bogunovic and D. Anselmetti, Electrophoresis **32** (17), 2253 (2011).

[11] B. Çetin and D. Li, Electrophoresis **32** (18), 2410 (2011).

[12] Z. R. Gagnon, Electrophoresis **32** (18), 2466 (2011).

[13] R. Pethig, L. M. Jakubek, R. H. Sanger, E. Heart, E. D. Corson and P. J. S. Smith, IEE Proc. Nanobiotechnology **152** (6), 189 (2005).

[14] H. P. Schwan, Adv Biol Med Phys **5**, 147 (1957).

[15] X. B. Wang, Y. Huang, P. R. Gascoyne, F. F. Becker, R. Holzel and R. Pethig, Biochim Biophys Acta **1193** (2), 330 (1994).

[16] U. Lei, P.-H. Sun and R. Pethig, Biomicrofluidics **5** (4), 044109 (2011).

[17] F. H. Labeed, J. Lu, H. J. Mulhall, S. A. Marchenko, K. F. Hoettges, L. C. Estrada, A. P. Lee, M. P. Hughes and L. A. Flanagan, PLoS ONE **6** (9), e25458 (2011).

[18] A. Downes, R. Mouras, P. Bagnaninchi and A. Elfick, J. Raman Spectroscopy **42** (10), 1864 (2011).

[19] I. Notingher, I. Bisson, A. E. Bishop, W. L. Randle, J. M. P. Polak and L. L. Hench, Anal. Chem. **76** (11), 3185 (2004).

[20] J. W. Chan, D. K. Lieu, T. Huser and R. A. Li, Anal. Chem. **81** (4), 1324 (2009).

[21] I.-F. Cheng, H.-C. Chang, D. Hou and H.-C. Chang, Biomicrofluidics **1** (2), 021503 (2007).

[22] V. Andrés and K. Walsh, J. Cell Biol. **132** (4), 657 (1996).

[23] K. E. Kamm and J. T. Stull, J. Biol. Chem. **276** (7), 4527 (2001).

[24] S. Fiedler, S. G. Shirley, T. Schnelle and G. Fuhr, Anal Chem **70** (9), 1909 (1998).

[25] T. Müller, G. Gradl, S. Howitz, S. Shirley, T. Schnelle and G. Fuhr, Biosensors and Bioelectronics **14** (3), 247 (1999).

[26] X. Hu, P. H. Bessette, J. Qian, C. D. Meinhart, P. S. Daugherty and H. T. Soh, PNAS **102** (44), 15757 (2005).

[27] U. Kim, J. Qian, S. A. Kenrick, P. S. Daugherty and H. T. Soh, Anal. Chem. **80** (22), 8656 (2008).

[28] S. Burgarella, S. Merlo, B. Dell'Anna, G. Zarola and M. Bianchessi, Microelectron. Eng. **87** (11), 2124 (2010).

[29] D. J. Morre and D. M. Morre, Biotechniques **7** (9), 946; 950; 956 (1989).

[30] H. Abdi, and L.J. Williams, Wiley Interdisciplinary Reviews: Computational Statistics 2, 433 (2010).

[31] D.J. Tritton, Physical fluid dynamics, 2nd ed., pp.206-213, Clarendon Press, Oxford (1988).

[32] C. Krafft, L. Neudert, T. Simat and R. Salzer, Spectrochim. Acta A: Molecular and Biomolecular Spectroscopy **61** (7), 1529 (2005).

[33] C. J. Frank, D. C. Redd, T. S. Gansler and R. L. McCreery, Anal Chem **66** (3), 319 (1994).

[34] J. R. Beattie, S. E. Bell, and B. W. Moss, Lipids **39**(5), 407 (2004).

[35] D. F. H. Wallach, S. P. Verma and J. Fookson, Biochim. Biophys. Acta - Reviews on Biomembranes **559** (2–3), 153 (1979).

[36] B. P. Gaber, P. Yager and W. L. Peticolas, Biophysical journal **24**(3), 677 (1978).

[37] C. J. de akker and P. M. Fredericks, Appl. Spectroscopy 49, 1766 (1995).

[38] W. H. Grover, A. K. Bryan, M. Diez-Silva, S. Suresh, J. M. Higgins and S. R. Manalis, PNAS **108**(7), 10992 (2011).

[39] N. G. Green and T. B. Jones, J. Phys. D: Appl. Phys. **40,** 78 (2007).

[40] H. Lizhi, K. Toyoda, and I. Ihara, J. Food Engineering 88, 151 (2008).

[41] W. Levin, Adv. Raman Spectrosc. 11, 1 (1984).

[42] B. J. Litman, E. N. Lewis, and I. W. Levin, Biochemistry 30(2), 313, (1991).

[43] B. Brügger, G. Erben, R. Sandhoff, F. T. Wieland, and W. D. Lehmann, PNAS 94, 2339 (1997).

[44] E. K. Fridriksson, .P. A. Shipkova, E. D. Sheets, D. Holowka, B. Baird, and F. W. McLafferty, Biochemistry 38, 8056 (1999).

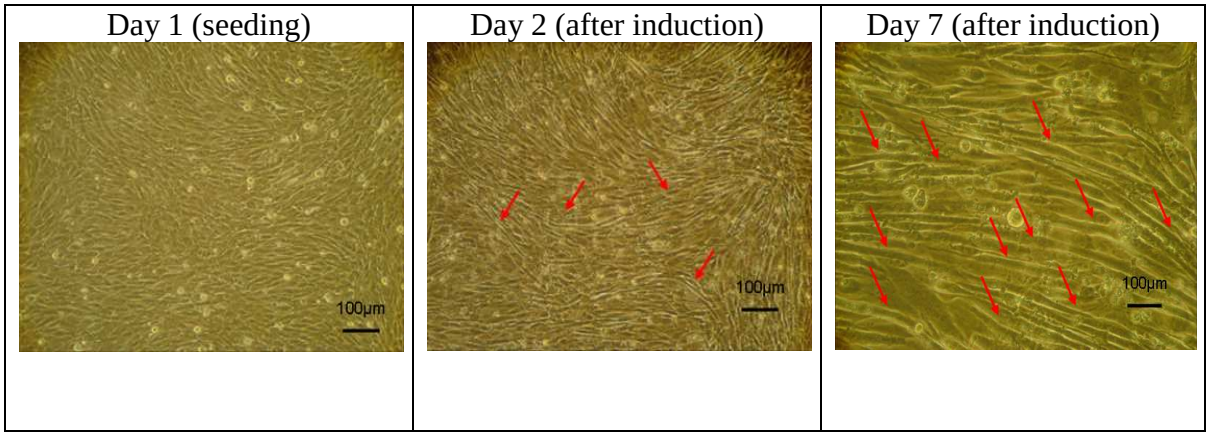

FIG. 1. Microscopic images (x20) of the C2C12 myoblasts at the first day of their seeding, and two stages (days 2 and 7) after their induction to form myotubes. The myotubes are indicated by arrows.

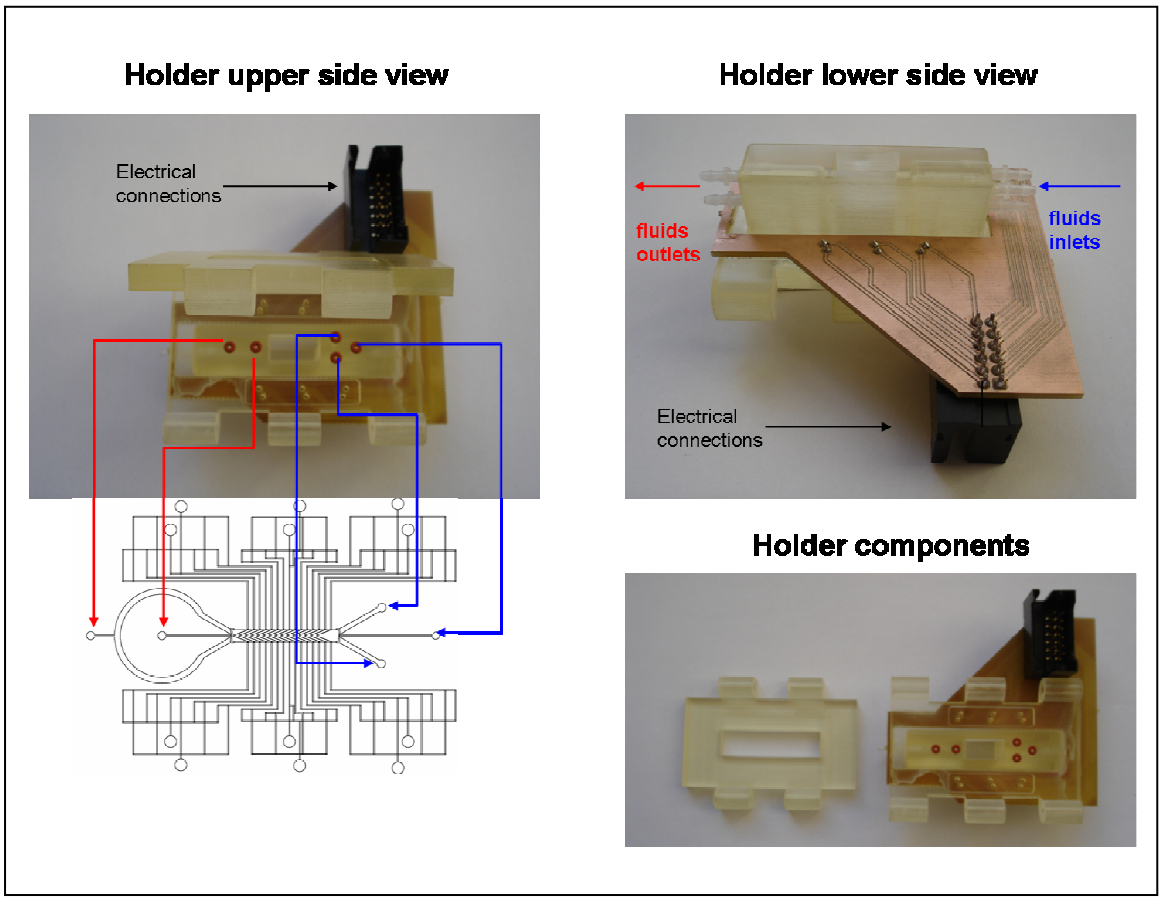

FIG. 2. Basic details of the DEP chamber and fluidic and electrical connections. See main text for details.

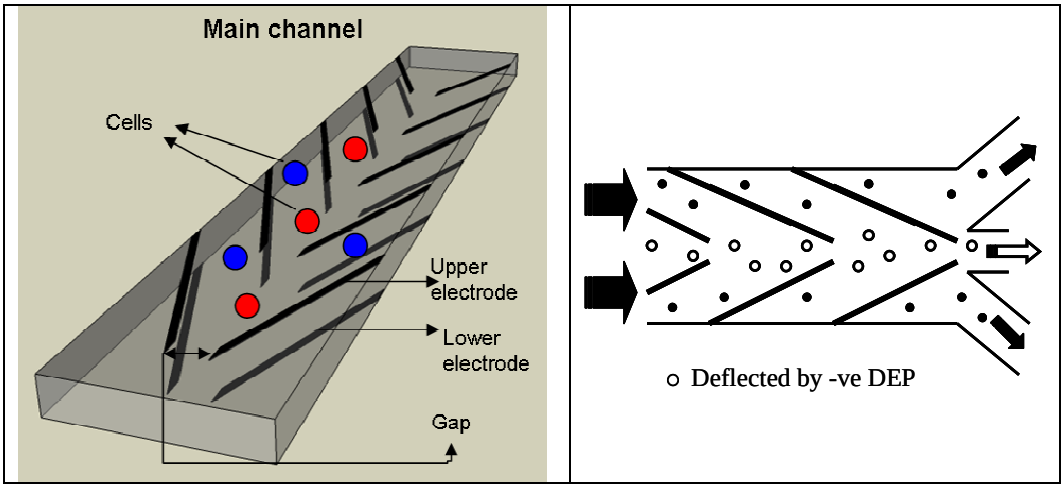

FIG. 3. Thirty electrodes (each 15 μm wide, spaced 500 μm apart, angled at 18^{o} to the fluid flow) were located along both the top and bottom surface of the DEP chamber to form a series of fifteen 3D electrode 'funnels'. The last set of five quadrupole electrodes are shown (left) with a gap of 50 μm between adjacent electrode tips. As shown (right) this facilitated the funnelling of cells deflected by negative DEP from the two outer fluid streams into the centre output fluid port.

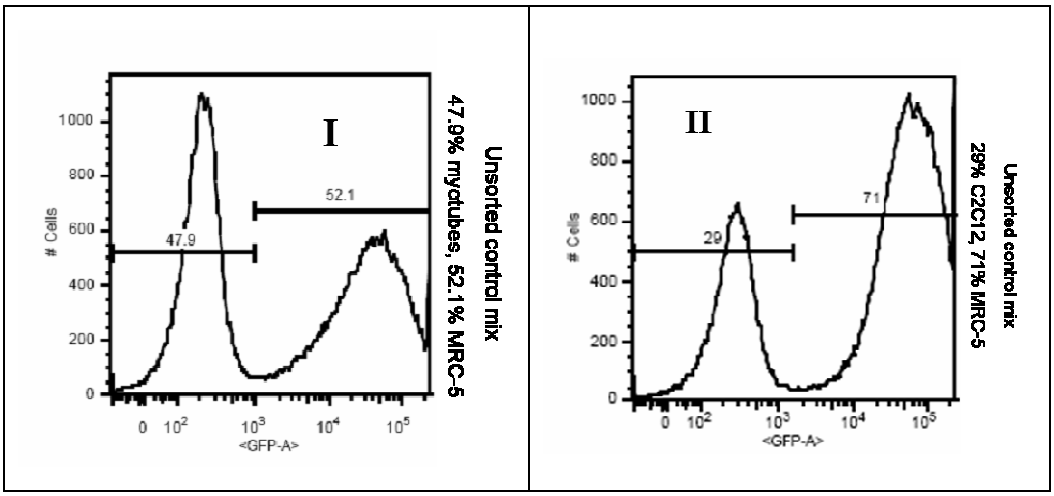

(a)

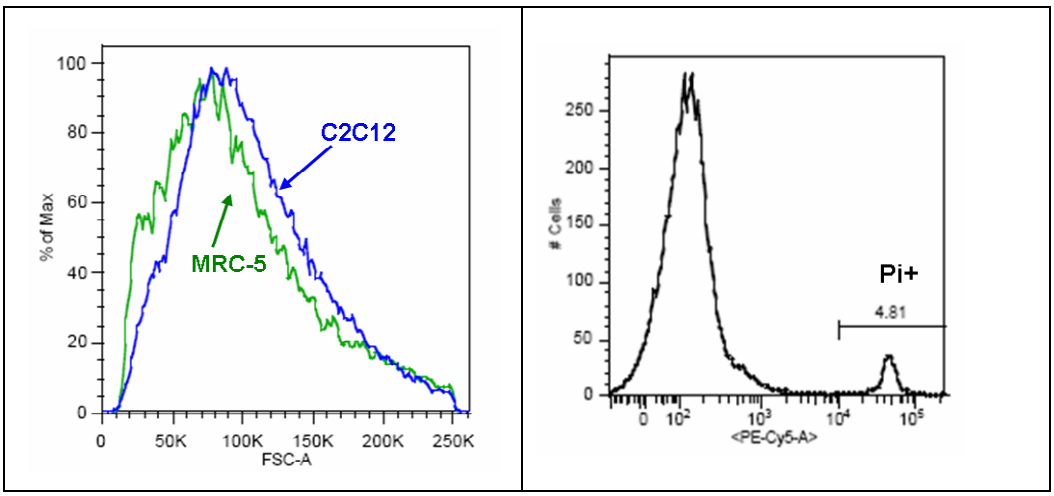

(b) (c)

FIG. 4. (a) Flow cytometry control experiments on cell samples (unsorted by DEP) to determine appropriate gate settings. (I) Myotubes mixed with MRC-5 GFP fibroblasts. (II) C2C12 cells co-cultured with MRC-5 GFP fibroblasts. (b) Superimposed forward scatter plots for (blue) C2C12 myoblasts (n = 59,518) and (green) MRC-5-GFP fibroblasts (n = 23,343). (c) Flow cytometry result for PI stained C2C12 myoblasts after DEP separation from myotubes, indicating 95.2% viability.

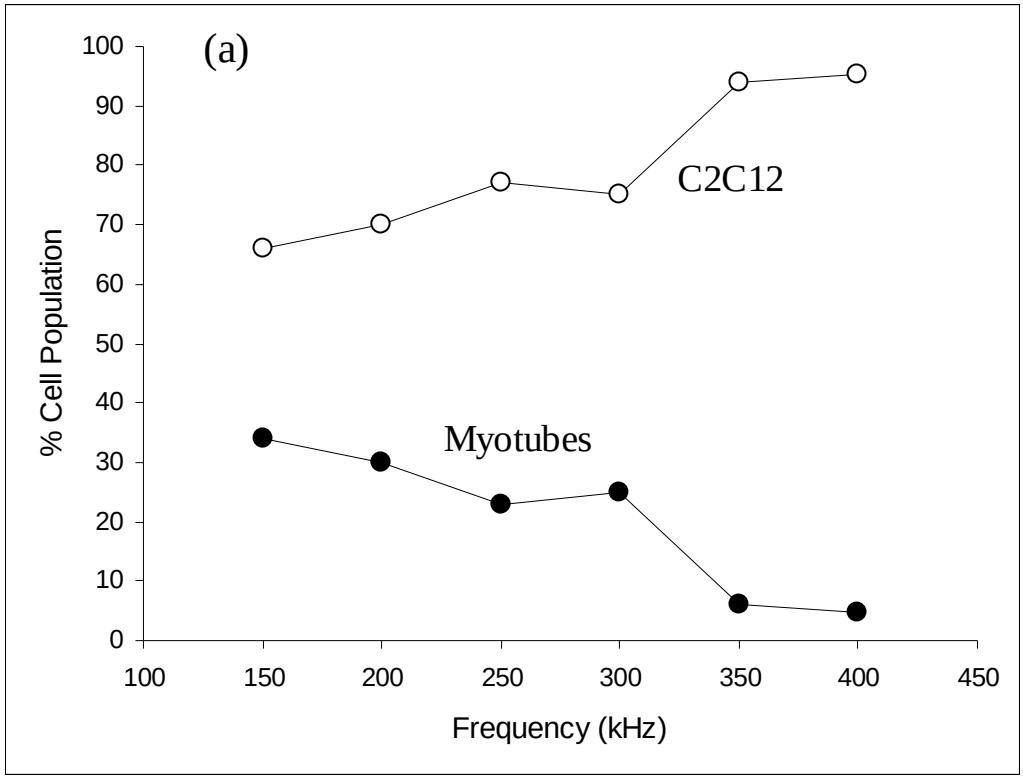

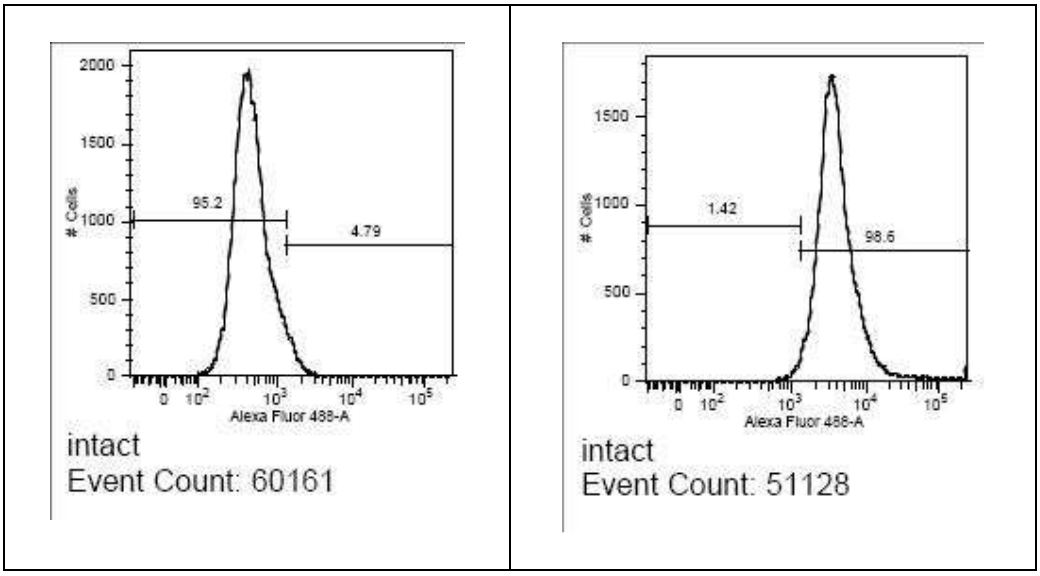

(b)

FIG. 5. (a) Flow cytometry analyses of a C2C12 sample (7 days after induction to myogenic differentiation) collected at 120 μl/hr from the central exit fluid port of the DEP chamber as a function of an applied 10 V(pk-pk) voltage frequency.
(b) Analyses of a sample separation at 409 kHz: (left) collection from central port (95.2% negative, 4.79% positive, for Alexa Fluor® 488); (right) collection from outer flow port (1.42% negative 98.6% positive, for Alexa Fluor® 488).

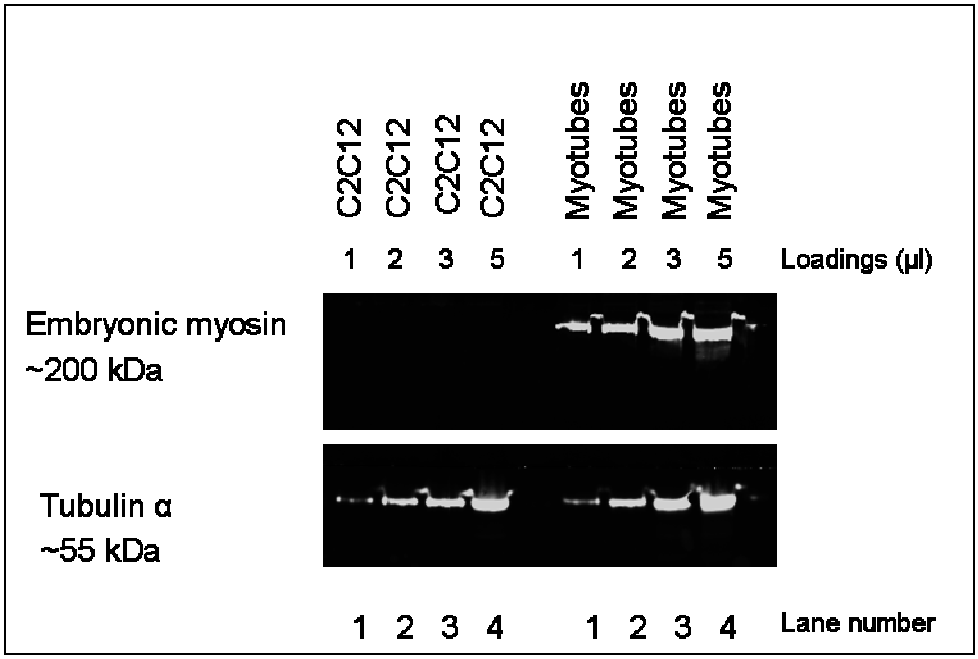

FIG. 6. Western blot analyses: C2C12 myoblasts and myotubes were separated by DEP at 409 kHz, and samples collected from the outer and centre fluid exit ports were blotted for embryonic myosin. The bands at ~200kDa (indicative of myotubes) were only present in the sample collected from the outer port, in agreement with the results shown in Figure 5. Tubulin was used to calibrate the protein loadings on the gel.

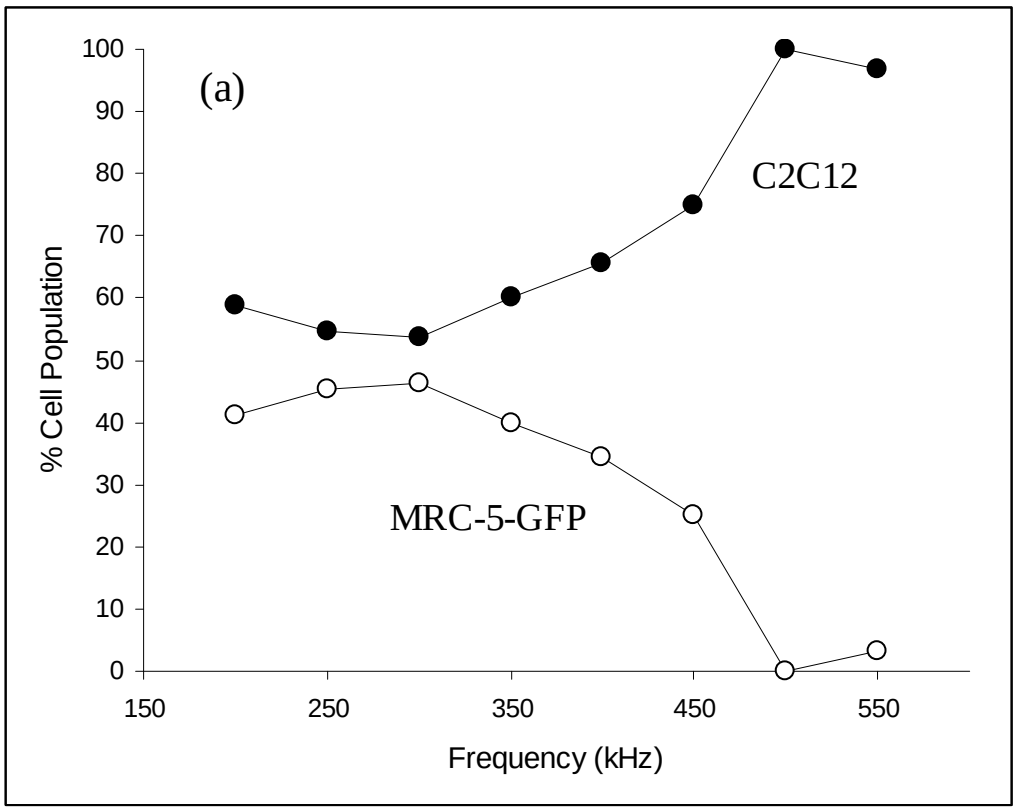

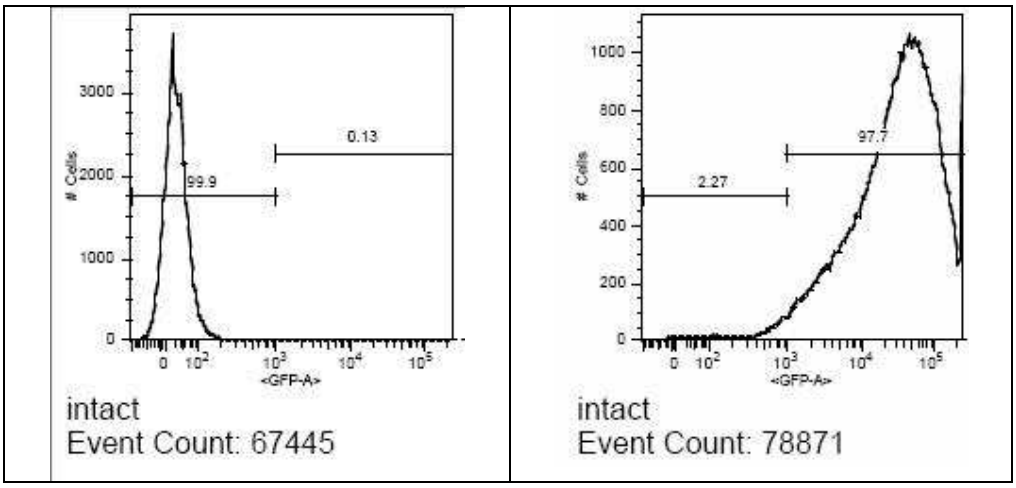

(b)

FIG. 7. (a) Flow cytometry analyses of a sample of C2C12 myoblasts co-cultured with MRC-5-GFP fibroblasts collected at 120 μl/hr from the central exit fluid port of the DEP chamber as a function of an applied 10 V(pk-pk) voltage frequency.
(b) Analyses of a sample separation at 500 kHz: (left) collection from central port (99.9% negative, 0.13% positive, for GFP); (right) collection from outer flow port (2.27% negative, 97.7% positive, for GFP).

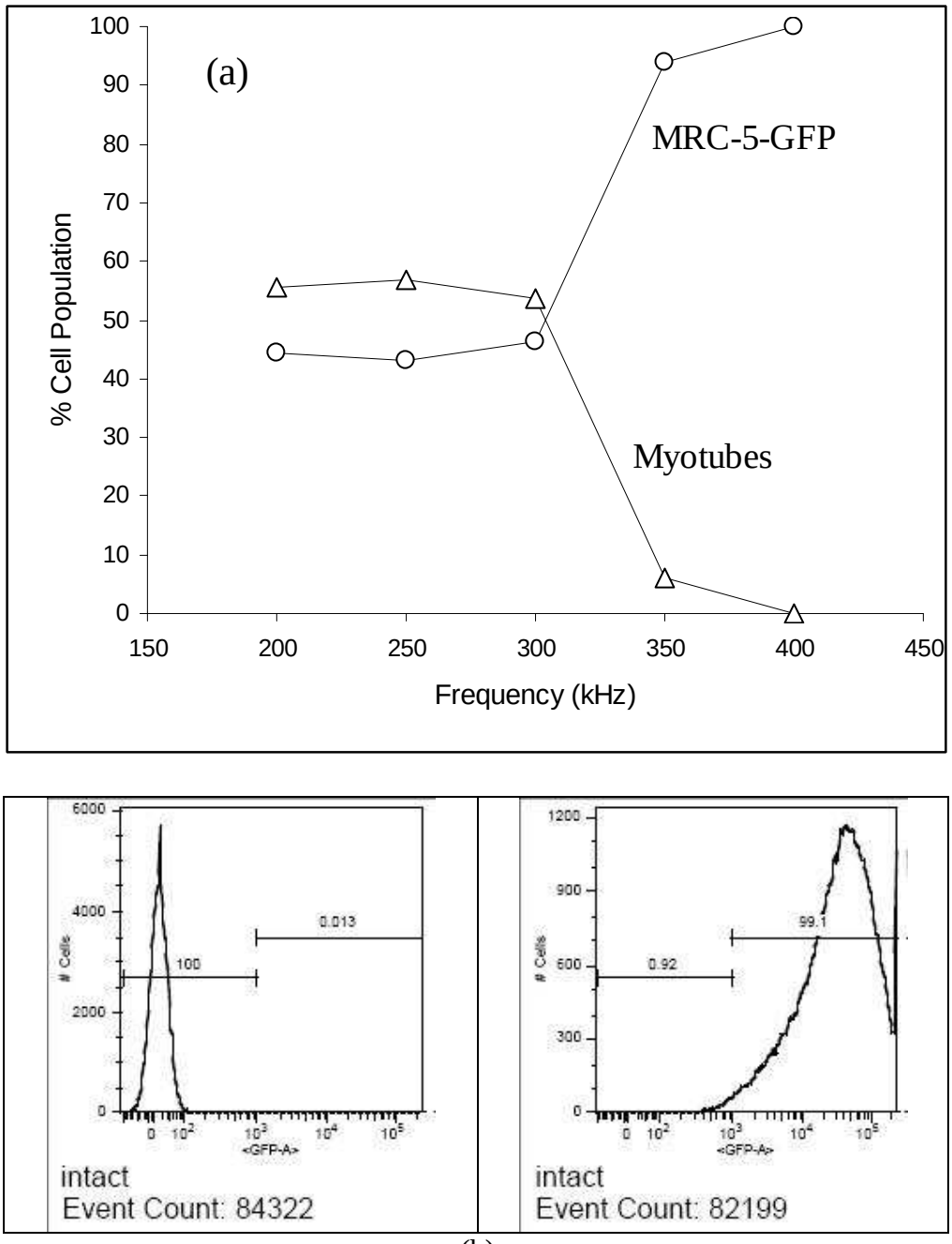

(b)

FIG. 8. (a) Flow cytometry analyses of mixed sample of myotubes and MRC-5-GFP fibroblasts collected at 120 μl/hr from the central exit fluid port of the DEP chamber as a function of an applied 10 V(pk-pk) voltage frequency.
(b) Analyses of a sample separation at 400 kHz: (left) collection from central port (100% negative, 0.013% positive, for GFP); (right) collection from outer flow port (0.92% negative, 99.1% positive, for GFP).

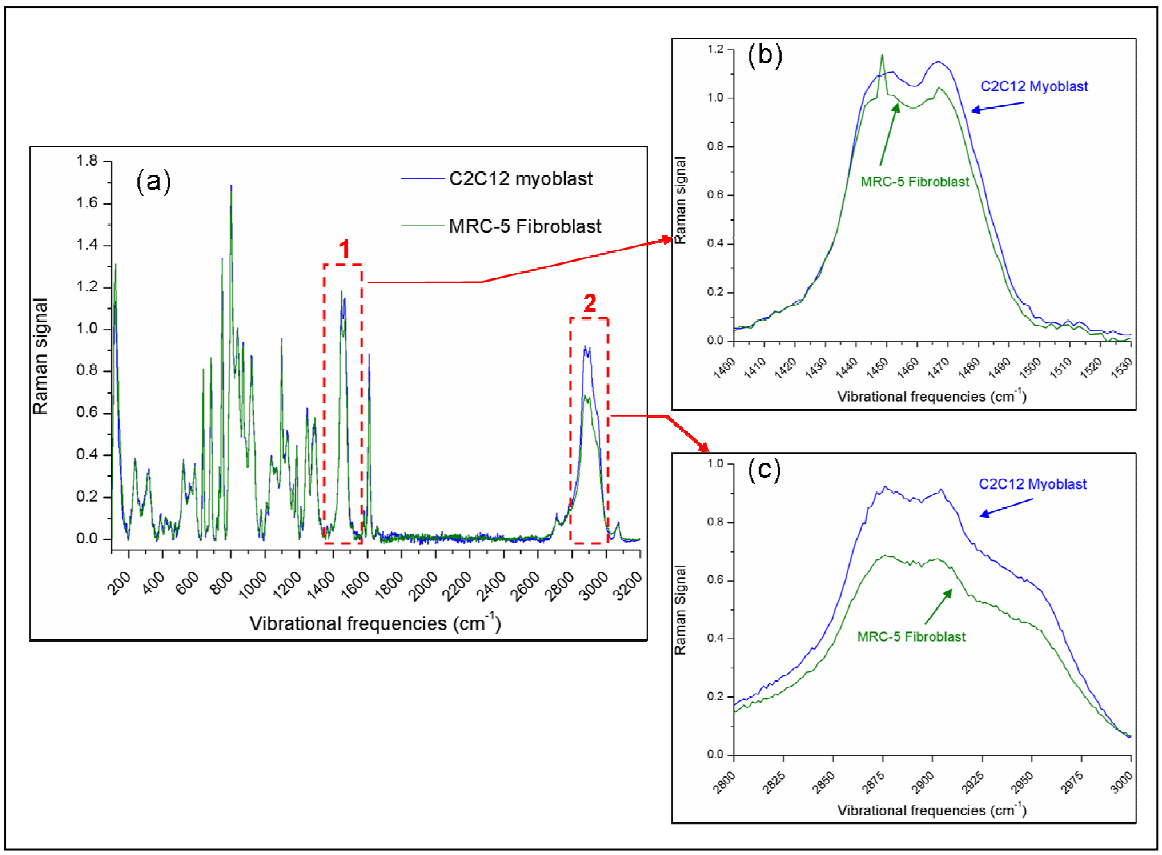

FIG. 9. (a) Normalised Raman spectra of cell membranes for C2C12 myoblasts and MRC5-GFP fibroblasts. Regions 1 and 2 correspond to CH_2 and CH_3 bending (1440, 1460 cm^{-1})[32, 33] and CH_2 stretching vibrations[34, 35] for saturated long CH chains (2860, 2840 and 2880 cm^{-1}), respectively. (b) Expanded region 1. (c) Expanded region 2. This data shows that the membranes of MRC5 fibroblasts have a lower proportion of saturated hydrocarbon bonds compared to C2C12 myoblasts.

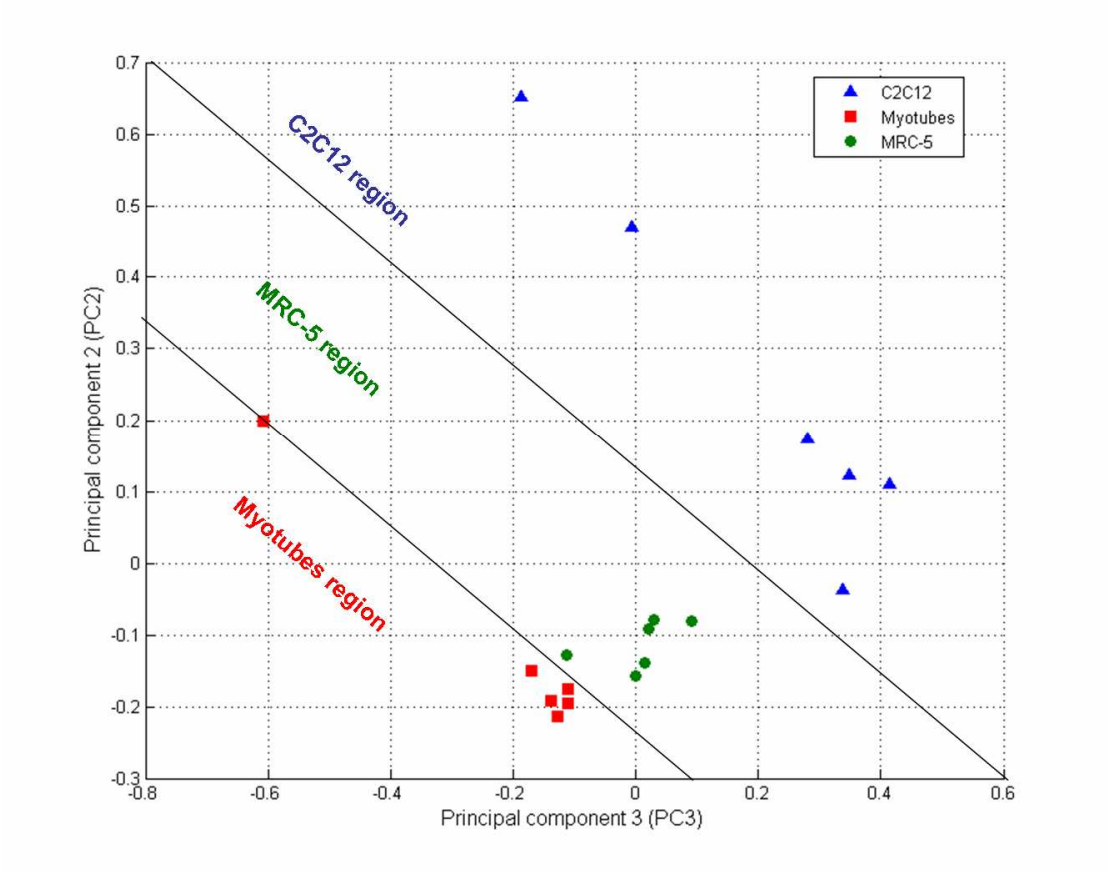

FIG 10. Scatter plot for the principal component analysis between PC3 and PC2. The PC3 loading gave the best separation of data between the three membrane types, and these are delineated by the two solid straight lines.

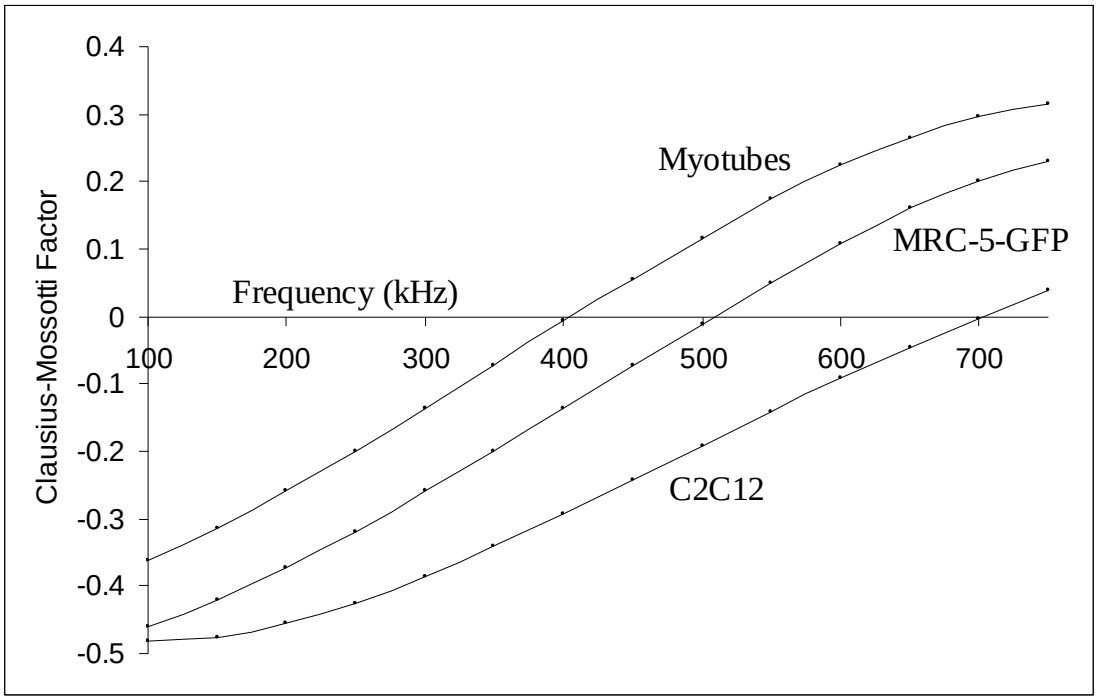

FIG. 11. MATLAB modelling of the Clausius-Mossotti polarizability factor for the three cell types, based on their estimated DEP crossover frequency values.